Available online at www.sciencedirect.com

SCIENCE DIRECT®

Polymer 46 (2005) 12511–12522

polymer

www.elsevier.com/locate/polymer

Reaction induced phase separation in mixtures of multifunctional polybutadiene and epoxy

Jaehyung Lee, Gregory R. Yandek, Thein Kyu *

Department of Engineering, Institute of Polymer Engineering The University of Akron, Akron, OH 44325, USA

Received 19 November 2004; accepted 6 January 2005

Available online 16 November 2005

Abstract

The phase behavior and separation dynamics have been investigated in blends of diglycidyl ether of bisphenol A (DGEBA), curing agent methylene dianiline (MDA), and a reactive liquid rubber (R45EPI) through application of differential scanning calorimetry (DSC), one- and two-dimensional light scattering, and optical microscopy. DSC analysis indicates that the system consists of three reactions: the self-condensations of DGEBA and R45EPI, as well as a cross-reaction between the two constituents. Observation of the dynamics of the 50/25.4/50 DGEBA/MDA/R45EPI system reveals that an initial phase separation is governed by the dominant self-curing reaction of DGEBA, followed by a phase dissolution characterized by a broadening of the interfacial regions catalyzed by a cross-reaction between the two species. A subsequent phase separation occurs at late stages since the copolymerization reaction does not proceed to completion. On the other hand, by changing the ratio of the beginning constituents to 70/25.4/30 DGEBA/MDA/R45EPI, the dissolution phenomena is not observed resulting from an even more dominant DGEBA/MDA condensation reaction. It is demonstrated that alterations in the initial compositional ratio greatly affect the phase separation dynamics of the system.

Keywords: Epoxy resin; Polymerization-induced phase separation; Copolymerization

1. Introduction

It is well known that brittle thermoset materials can be toughened by the incorporation of an elastomeric or thermoplastic additive [1–6]. In a previous paper, the dynamics of polymerization-induced phase separation (PIPS) have been examined for mixtures of diglycidyl ether of bisphenol A (DGEBA) and carboxyl-terminated butadiene acrylonitrile (CTBN), often known as liquid rubber, using methylene dianiline (MDA) as a curing agent [7]. During polymerization the upper critical solution temperature (UCST) curve moved to a higher temperature and concurrently shifted to a composition high in non-reactive liquid rubber. This asymmetric movement of the coexistence curve has been attributed to instabilities driven by the increase in molecular weight of the reacting prepolymer. The coexistence curve generally surpasses the reaction temperature at off-critical compositions thereby triggering phase separation in the metastable region where nucleation and growth (NG) is expected to dominate. In this region, small thermal fluctuations decay while leaving only a disproportionate amount of large fluctuations upon which growth occurs. With the progression of reaction, the continued increase in molecular weight further drives the system into the unstable region such that there occurs a crossover in behavior from NG to spinodal decomposition (SD). An intriguing observation is that the length scale was found to decrease during PIPS. One plausible account is the formation of new domains between the existing ones. Another possible account is that as the supercooling (i.e. the temperature difference between the coexistence point and the reaction temperature) increases with progressive reaction, the average domain size becomes smaller. This is consistent with the notion that the larger the supercooling, the smaller the domain size. However, this mechanism of length reduction is opposed by the coalescence of the domains due to thermal relaxation of the system, which favors the domain growth. The competition between the two opposing mechanisms would eventually determine the domain size and the mechanism(s) of PIPS dynamics such as NG or SD or their crossover processes. It can also be anticipated that the reduction of length scale may not be observable even in the early stage if the amount of curing agent were lowered, or the reaction temperature is increased

---

* Corresponding author. Tel.: +1 330 9726672; fax: +1 330 2582339.
E-mail address: tkyu@uakron.edu (T. Kyu).

0032-3861/$ - see front matter © 2006 Elsevier Ltd. All rights reserved.
doi:10.1016/j.polymer.2005.01.109

appreciably or the reactivity of the curing agents is lowered. In the intermediate to late stages, the coalescence of domains would prevail, thus the growth scaling exponents can be expected to be smaller as compared with those of the thermal quench induced phase separation (TIPS) case.

In this paper, we extend our study to a more complex case of the dynamics of reaction induced phase separation in mixtures of two reactive prepolymers with or without a curing agent. The non-reactive CTBN has been replaced by a reactive liquid rubber, viz., multifunctional polybutadiene (labeled R45EPI, i.e. liquid rubber having hydroxyl groups at the chain ends and epoxide groups in the middle of chains). R45EPI molecules have the ability to react among themselves or with DGEBA in the absence of any curing agents. Phase behavior, isothermal curing kinetics, dynamics of PIPS, and structure development have been examined on the basis of differential scanning calorimetry (DSC), time-resolved light scattering, and optical microscopy. Of particular interest is an initial phase separation, followed by a phase dissolution and subsequent secondary phase separation.

2. Materials and experiments

Diglycidyl ether of bisphenol-A (DGEBA), known as Epon 828, was supplied by Shell Chemicals, and the hydroxyl-terminated polybutadiene (R45EPI) was supplied by Nagase & Co., Ltd. The chemical structures of these prepolymers as well as the curing agent MDA are depicted in Fig. 1. All blend samples were prepared by dissolving in solvent, namely tetrahydrofuran (THF), followed by casting on slides or in DSC pans and subsequent vacuum drying for a minimum of 72 h.

Phase separation induction times were measured monitoring the scattering intensity at a fixed angle (ca. 10°) using an HC-220-01 photodiode detector manufactured by Hamamatsu Co. A 2 mW He–Ne laser supplied by (Model LSR2R, Aerotech Inc.) with a wavelength of 632.8 nm was used as the light source. The temperature of the sample-heating block was regulated by a Model 2010 Omega controller with an accuracy of ±0.5 °C. A one-dimensional silicon diode reticon detector (Model 1453, Princeton Applied Research (PAR) coupled with an optical multi-channel analyzer (Model 1460, OMA III, PAR) was used to measure scattering profiles. Two-dimensional scattering profiles were obtained from a CCD camera (Model 1461, EG&G PAR), connected to a WEF-488 interface (Model 1461, EG&G PAR). Optical microscopy (OM) was performed on a Nikon OPTIPHOT2-POL) with a Nikon UFX-DX camera. Differential scanning calorimetry (DSC) was performed on a Dupont thermal analyzer, Model 9900, at a heating rate of 20 °C/min unless indicated otherwise.

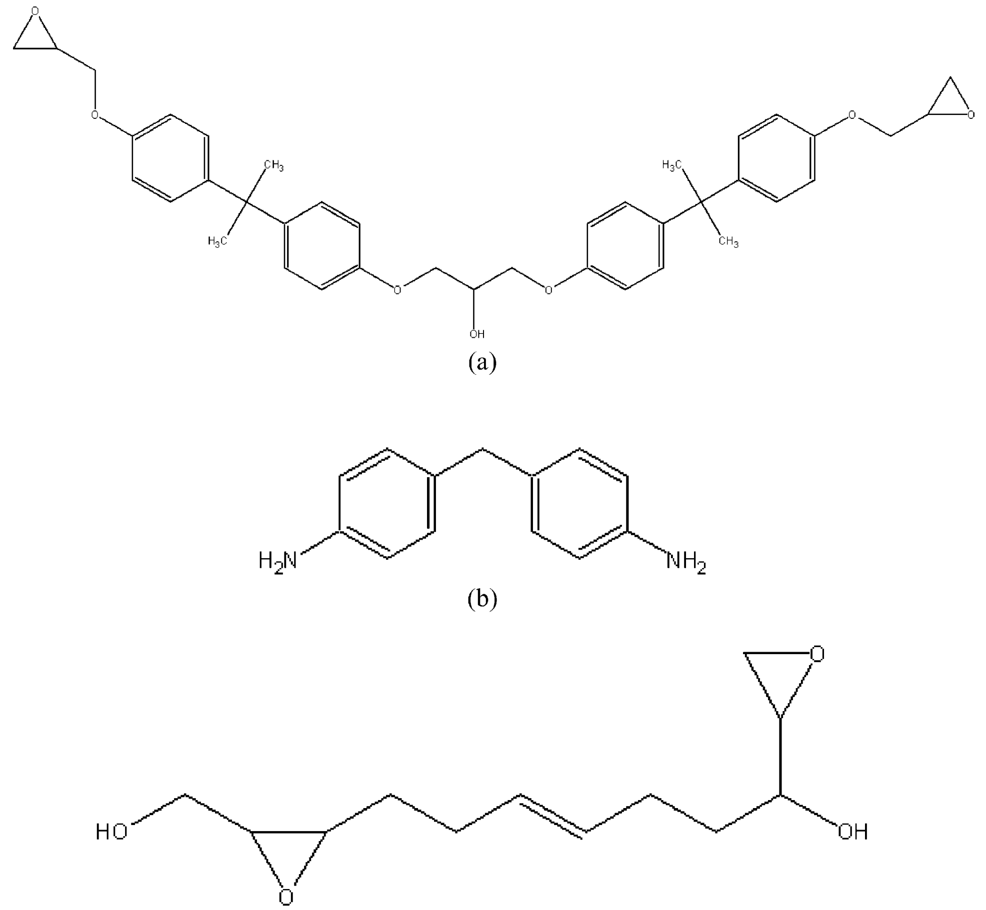

(a)

(b)

(c)

Fig. 1. Chemical structures of (a) DGEBA, (b) MDA, and (c) R45EPI.

3. Results and discussion

3.1. Thermal investigations of miscibility and reaction kinetics

The DGEBA/R45EPI mixtures appear transparent to the naked eye and show no identifiable texture under microscopic investigation. These blends scatter no light in the cloud point measurement, suggestive of a favorable interaction between the pair. DSC scans indicate that the DGEBA/R45EPI mixtures possess a single glass transition temperature (T_g) exhibiting a nonlinear dependence on composition from −70 to −12 °C (Fig. 2(a)). Such a trend in T_g is characteristic of miscible pairs [8]. The probable miscibility of the DGEBA/R45EPI blends may be partially due to the low molecular weights of the constituent prepolymers. If the coexistence curve were to exist, it would be of an upper critical solution temperature type with a convex maximum below room temperature.

In light of the fact that the neat multifunctional polybutadiene (R45EPI) contains hydroxyl groups at the chain ends and epoxide groups in some intermediate positions of the chain, R45EPI is self-curable. Upon blending with DGEBA, the hydroxyl groups located at the ends of R45EPI molecules would react favorably with the epoxide groups of DGEBA rather than with its own epoxide groups because of the steric hindrance that would favor the interchain reaction over the intrachain reaction. Another interesting point is that when a curing agent is added to the blends, reactivities amongst the involved species may not be the same since the reaction rate strongly depends on functionality, reaction temperature, and amount of curing agent.

Temperature-sweep DSC scans for various DGEBA/R45-EPI mixtures absent of curing agent at a temperature range of 50–300 °C are displayed in Fig. 2(b). In the neat R45EPI, a single curing peak appears with a maximum located at 205 °C that characterizes its self-condensation reaction, while as expected, the neat DGEBA exhibits no curing peak in the investigated temperature range. Interestingly, the intermediate blends show two characteristic peaks which may be attributed to a cross-reaction between the constituent components since DGEBA is not capable of reacting with itself. The existence of

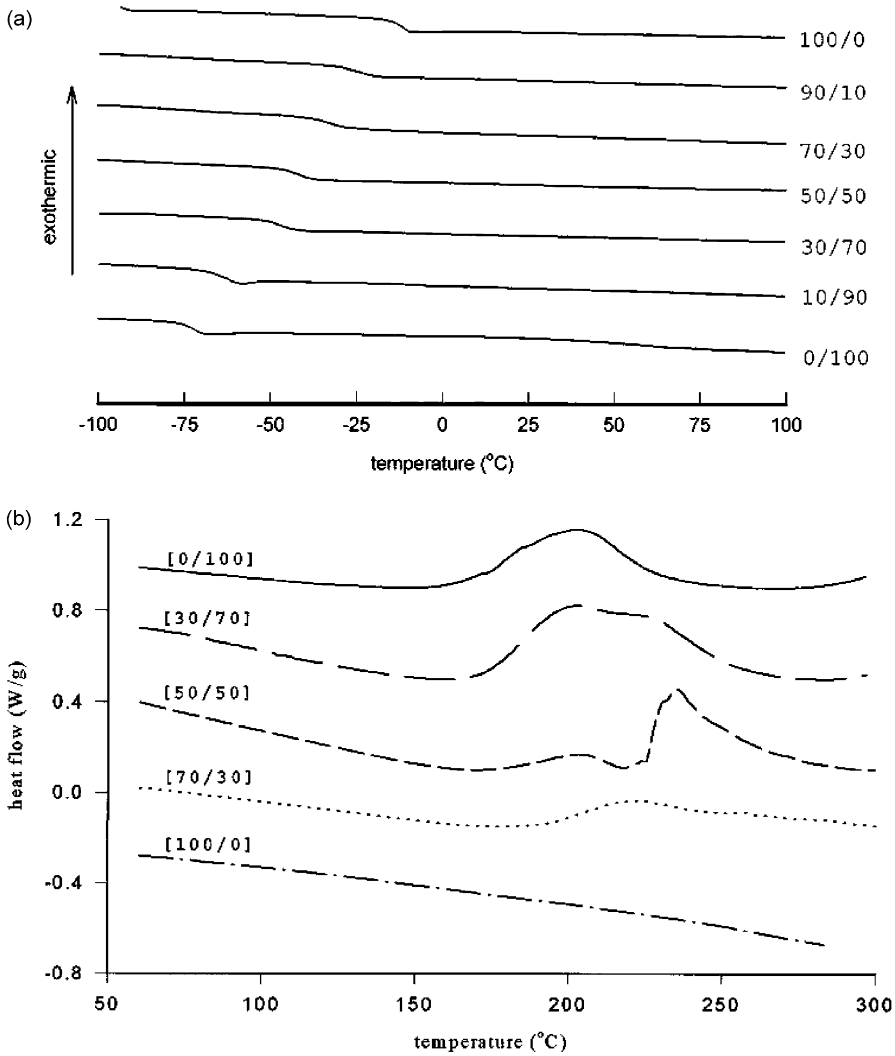

Fig. 2. (a) DSC scans of DGEBA/R45EPI blends in the temperature range of −100 to 100 °C, showing a systematic movement of T_g suggestive of a miscible character of the pair. (b) DSC thermograms of DGEBA/R45EPI blends in the temperature range of 50 to 300 °C. The scan rate was 20 °C/min.

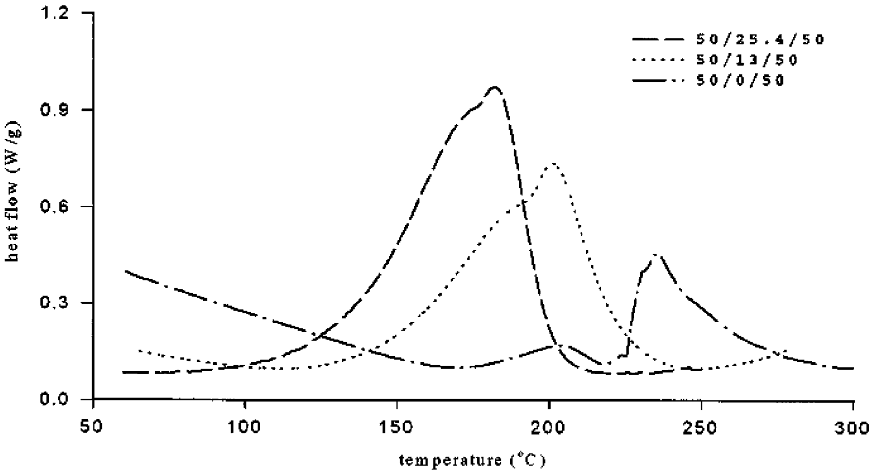

Fig. 3. DSC thermograms of 50/50 DGEBA/R45EPI mixtures with various amounts of MDA. The scan rate was 20 °C/min.

this reaction is further corroborated by the realization that the second peak is most pronounced in the 50/50 blend, which exhibits complete separation from the R45EPI peak with a maximum located at a higher temperature of approximately 235 °C. It should be further noted that the heat of reaction for the cross-reaction is much more significant than the self-curing reaction of the pure R45EPI, revealing that the reactive liquid rubber preferentially reacts with epoxy over itself.

To elucidate the role of MDA in the blends, DSC scans of three different compositions ranging from zero to equivalent amount of the curing agent for the 50/50 DGEBA/R45EPI mixtures are shown in Fig. 3. Considering the 50/0/50 DGEBA/MDA/R45EPI blend, two exothermic peaks are observed: a smaller peak with a maximum located at 205 °C characterizes the self-condensation reaction of R45EPI while the much larger peak at a higher temperature of 235 °C is clearly attributed to a cross-reaction between DGEBA and R45EPI since no hardener is present. Two interesting trends are evident from the DSC thermograms. First, as the amount of curing agent increases, the heat of reaction of the secondary peak decreases. This behavior may be attributed to an increase in collisions between DGEBA and curing agent molecules resulting in a lower probability of reacting with R45EPI molecules. Second, the location of the cross-reaction peak shifts towards lower temperatures with increasing levels of curing agent, implying that the aforementioned cross-reaction may be catalyzed by MDA, thereby occurring at lower temperatures.

Additional peculiar features for these blend systems may be discerned from the DSC scans at an approximately constant loading level of curing agent MDA (Fig. 4). Most noteworthy is the observance of an incomplete but substantial suppression of the self-condensation reaction of R45EPI in the presence of MDA, i.e. 7.85 J/g with respect to R45EPI weight. This total heat of reaction is a mere one-ninth that of the heat of reaction of the self-condensation of R45EPI without MDA. Another peculiarity is that a small additional peak is observable in the 50/25.4/50 DGEBA/MDA/R45EPI mixture. This secondary

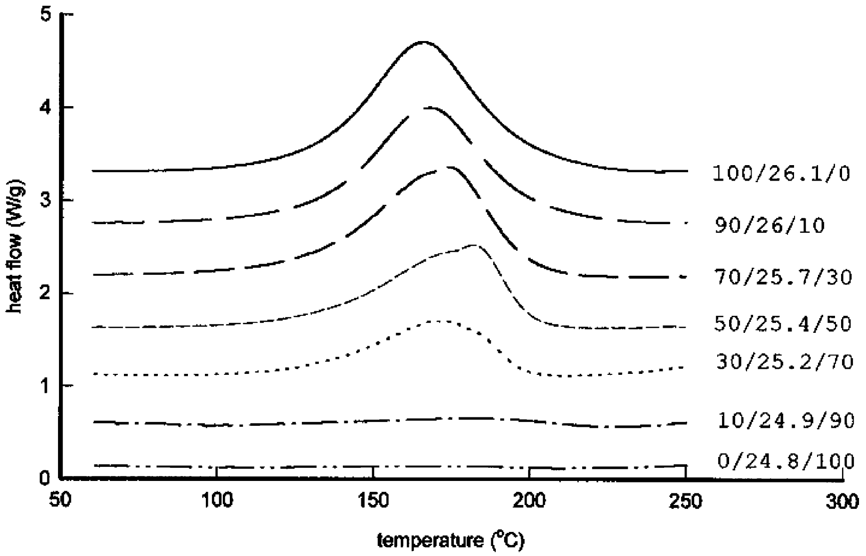

Fig. 4. DSC thermograms of various DGEBA/R45EPI mixtures with an equivalent amount of curing agent, MDA. The scan rate was 20 °C/min.

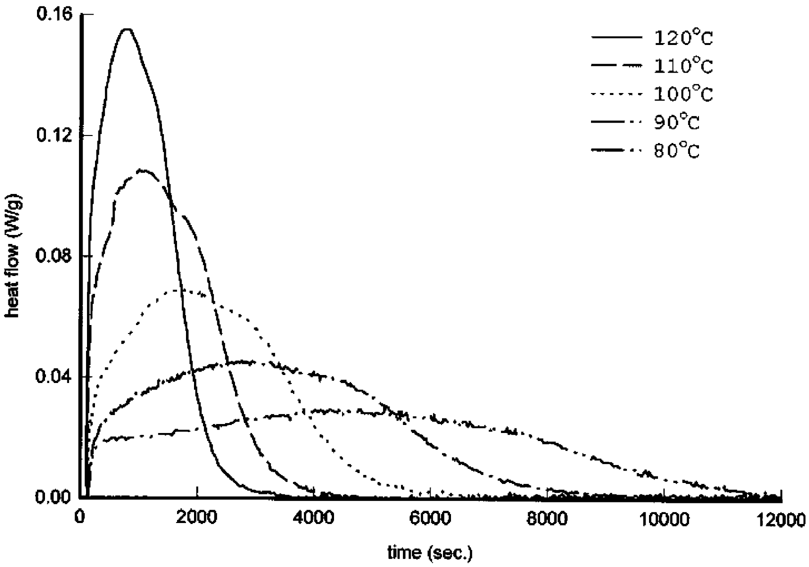

Fig. 5. The rate of heat generation in DGEBA/MDA/R45EPI (50/25.4/50) blends as a function of curing time at the indicated temperatures.

peak presumably arises from a reaction between DGEBA and R45EPI chains since the self-curing of R45EPI is suppressed in the presence of MDA. The heat of cross-reaction is not observable in the other blends, or it may be insignificant in comparison to the reaction of epoxy with curing agent, possibly being overshadowed by those peaks.

Further evidence supporting the existence of a cross-reaction is suggested by close examination of the isothermal DSC scans showing heat generation at five different temperatures for the DGEBA/MDA/R45EPI (50/25.4/50) mixture (Fig. 5). Each curve with the exception of one at 80 °C shows a small inflection (shoulder) representing the reaction between DGEBA and R45EPI. It is evident from these sets of DSC data that three possible conclusions may be derived: first, MDA suppresses the self-condensation of R45EPI; second, R45EPI preferentially reacts with DGEBA over itself; lastly, the epoxy/hardener reaction is dominant over the cross-reaction, especially with increased levels of curing agent.

3.2. Concentration effect on the dynamics of phase separation

Fig. 6 depicts the intensity variation with reaction time for two different compositions at 100 °C. As witnessed in Fig. 6(a), the 70/25.7/30 mixture shows a sudden increase in intensity at approximately 33 min, then leveling off at 75 min. During the course of polymerization, the molecular weight of DGEBA increases causing the system to become unstable, which in turn raises the coexistence curve to a higher temperature. When the coexistence curve surpasses the experimental temperature, light scattering occurs due to an increase in concentration fluctuations. An abrupt increase in the scattered light intensity at a threshold time may be characterized as the induction time (t_{ip}). In Fig. 6(b), the 50/25.4/50 mixture exhibits an abrupt increase in the scattered light intensity at 52 min. Subsequently, the intensity declines rapidly and then slowly increases again in comparison with the first increase. The first onset of the intensity rise is taken as the t_{ip}. The interpretation of this unusual intensity variation for the 50/25.2/50 mixture will be performed later in this paper.

It may be hypothesized that the induction time for phase separation is solely dependent on the rate of the dominant chemical reaction, in this case the condensation of epoxy with

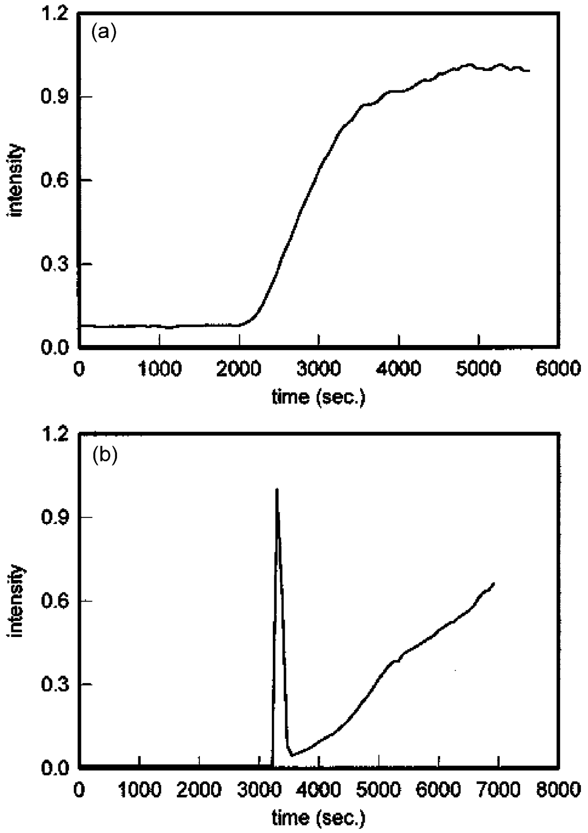

Fig. 6. Temporal change of scattered intensity at a fixed angle of 20° for DGEBA/MDA/R45EPI mixtures at 100 °C. (a) 70/25.7/30 and (b) 50/25.4/50.

MDA. This is of our intuition that the coexistence curve of the phase diagram progressively shifts upward owing to a reduction in the entropic contribution of the free energy as the molecular weight of the reactive species increases with reaction. The experimental point eventually falls within the bounds of the coexistence region due to this temporally dependent shift. Specifically, as the curing rate increases with temperature, the induction time is consequently reduced. Furthermore, as the initial composition of DGEBA in the initial mixture is increased, the reaction rate is also expedited, resulting in a notable decline of the phase separation induction time. A comparison of t_{ip} between the 50/25.4/50 and 70/25.7/30 results in an approximate 22 min decrease for the blend of higher DGEBA content at 90 °C, although the induction times for the two mixtures exhibit less difference at higher reaction temperatures (i.e. 5 min at 120 °C).

At 100 °C, the time evolution of the light scattering peaks for the DGEBA/MDA/R45EPI (70/25.7/30) mixture reveals that the scattering intensity increases with time after 34 min while the location of the scattering maximum does not change significantly through the course of the phase separation (data not shown). A similar experiment was undertaken for two additional temperatures of 120 and 140 °C. At these higher temperatures, there is a definite movement of the scattering peak to lower scattering angles. The scattering maxima, q_{m}, are plotted according to the power law form against time, $t - t_{\mathrm{ip}}$ in Fig. 7. The temporal evolution in the 120 °C case is complex; i.e. q_{m} increases initially, then it declines for some intermediate period, and eventually levels off due to chemical pinning. At 140 °C, it is apparent that q_{m} decreases with time with an exponent of approximately $-1/5$ and subsequently chemical pinning takes place due to crosslinking. These results are reminiscent of those observed in the DGEBA/MDA/CTBN 90/12/10, 80/21/20, and 70/18.3/30 mixtures at relatively high temperatures (120 and 160 °C) [7].

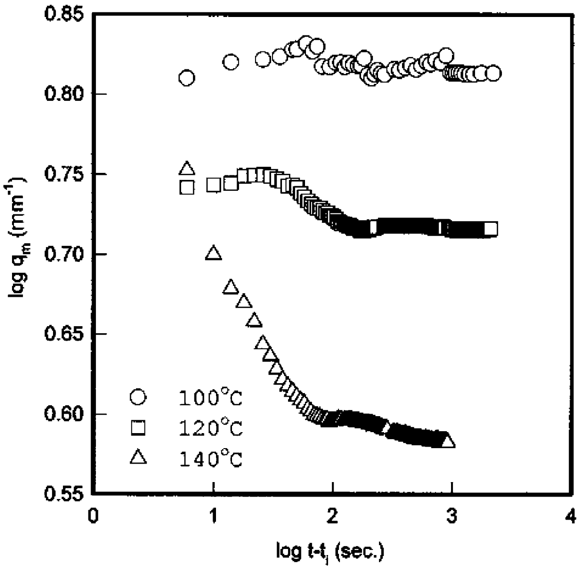

Fig. 7. Log–log plot of maximum wavenumber q_{m} vs. time ($t - t_{\mathrm{ip}}$) for the DGEBA/MDA/R45EPI 70/25.4/30 mixture at various temperatures.

As discussed earlier, the increase in molecular weight of the reactive species will expand the envelope of the coexistence region continuously such that the experimental point is pushed into deeper quenching with time possibly passing into and through the metastable and unstable regions. It is well known that in the metastable regions of phase diagrams, nuclei form if large enough concentration fluctuations exist; however, these fluctuations may be suppressed by the formation of a three-dimensional network resulting from the chemical crosslinking reaction, thus the number of nuclei formed may be extremely limited. In the unstable or spinodal regime, nuclei formed in the nucleation regime may be the triggers of spinodal instability. According to mean-field theory, as the experimental point moves to deeper quenching in the spinodal regime, the correlation length ξ may be related to the quench depth as follows [6]:

$$\xi(t) \sim (\chi_{\mathrm{c}} - \chi)^{-1} \sim (\Delta T)^{-1} \tag{1}$$

where χ_{c} is the critical value of the interaction parameter that changes with time. Eq. (1) predicts that as the coexistence region shifts towards higher temperatures with the increase in molecular weight of the polymerizing component, the correlation length for the system decreases because of the increase in ΔT. A natural result of Eq. (1) is the dependence of the scattering maximum q_{m} on the quench depth, i.e.

$$q_{\mathrm{m}}(t) = \xi(t)^{-1} \sim \Delta T \tag{2}$$

Contrary to the typical growth exhibited by the thermally quenched case where the correlation length increases (scattering maxima decrease) with time, the present reaction-induced phase separation demonstrates scattering maxima that shift to larger scattering angles with time. This unusual behavior has been previously explained by attributing it to the fact that newer domains are created between the previously formed domains, corresponding to the metastable region where heterogeneous nucleation occurs. With continued reaction, the system transits from metastable to unstable regimes [7].

Strictly speaking, the domains thus formed are affected by a competition between both the size reduction due to increased supercooling (i.e. higher ΔT), and structure relaxation due to the thermal-induced effect contributing to their growth. The thermally induced growth behavior has been well described by the scaling law [9–19] in which the structural growth due to thermal relaxation obeys the following forms [13,14]:

$$q_{\mathrm{m}}(t) \sim t^{-\alpha} \tag{3}$$

$$I_{\mathrm{m}}(t) \sim t^{\beta} \tag{4}$$

where the growth exponents, α and β, are 1/3 and 1 in the cluster limit, and 1 and 3 in the percolation limit where hydrodynamics dominate, respectively. However, in the PIPS case, regarding the growth of the scattering maximum in Eq. (3), the wavelength selection rule predicts a smaller value of 1/4, which may actually vary between $-1/2$ and 1 depending on the reaction rate [6]. The overall scaling of the domain growth is therefore a consequence of the coupling of (i) the continuous quenching of the experimental temperature, which yields an increase in q_m as described by Eq. (2), and (ii) the gradual growth of the structure due to thermal relaxation, described by Eq. (3) depending on the stage of the phase separation. These types of growth are illustrated in Fig. 8 according to the location of the experimental point on the phase diagram. This competition phenomenon has been termed nucleation-initiated spinodal decomposition (NISD), where there is a crossover in phase separation behavior from nucleation-growth to spinodal decomposition as the critical point shifts to higher temperatures [7]. Except for the critical or near-critical compositions, phase separation is generally initiated in the metastable region, where nucleation would dominate. With the progression of the reaction, the system may be further thrust into the unstable region where phase separation is dominated by spinodal decomposition.

A schematic explanation of the coupling between the aforementioned mechanisms such as size reduction due to increased supercooling and the growth due to thermally induced structure relaxation of the domains is shown in Fig. 9. If the quenching effect on q_m due to the progressive movement of the coexistence curve towards higher temperatures is strong enough to suppress structure relaxation, i.e. the rate of polymerization is faster than that of phase separation, the overall scaling of q_m may be represented as in Fig. 9(a). In this case q_m increases with time and the resultant structures are small in size. Furthermore, concentration fluctuations do not have the opportunity to reach the equilibrium values governed by the thermodynamics of the system. On the other hand, if the movement of the coexistence curve is slow such that the system has the opportunity to relax, the quenching effect is reduced, and the time dependence of the q_m may be

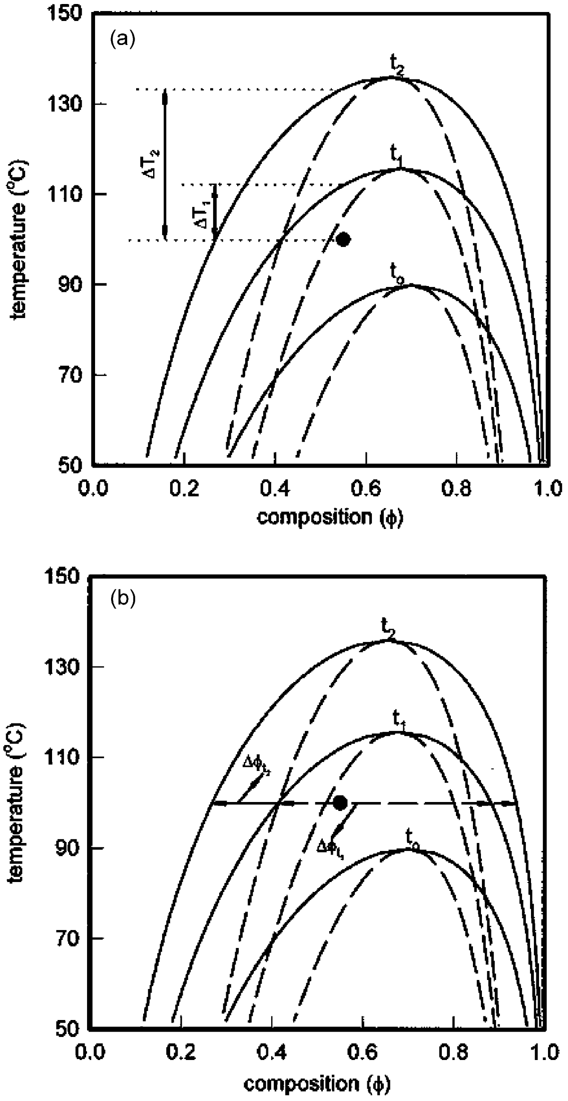

Fig. 8. Hypothetical temporal change of an upper critical solution temperature (UCST) associated with progressive polymerization of component 2, demonstrating (a) the size reduction due to supercooling effect and (b) coarsening effect due to thermally induced effect.

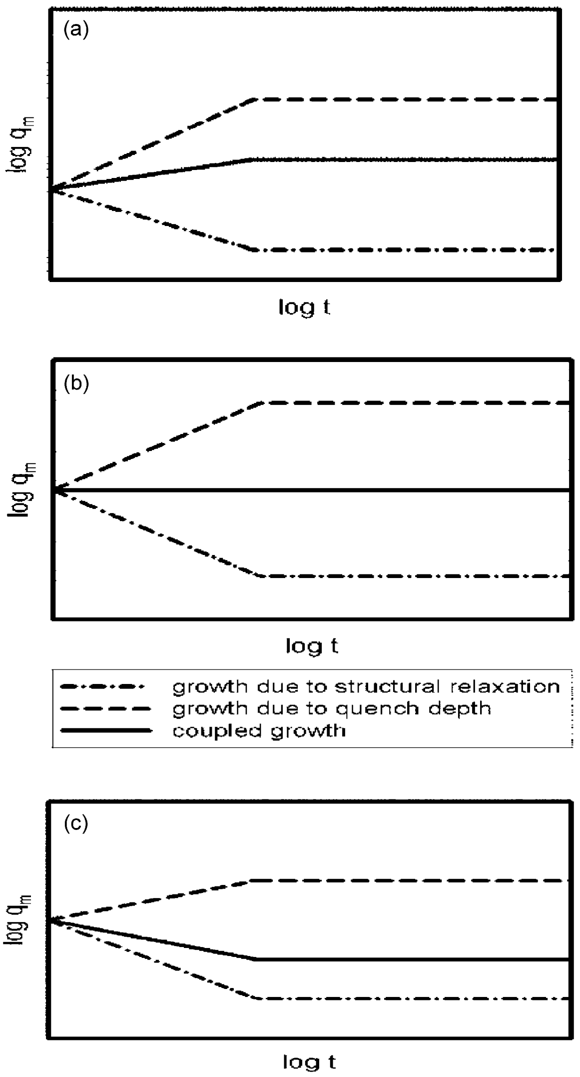

Fig. 9. Schematic drawing of the domain growth: (a) supercooling effect (ΔT) being dominant in the early stage, (b) supercooling effect being balanced with structure relaxation in the early stage, and (c) structure relaxation dominating over the supercooling effect in the early stage.

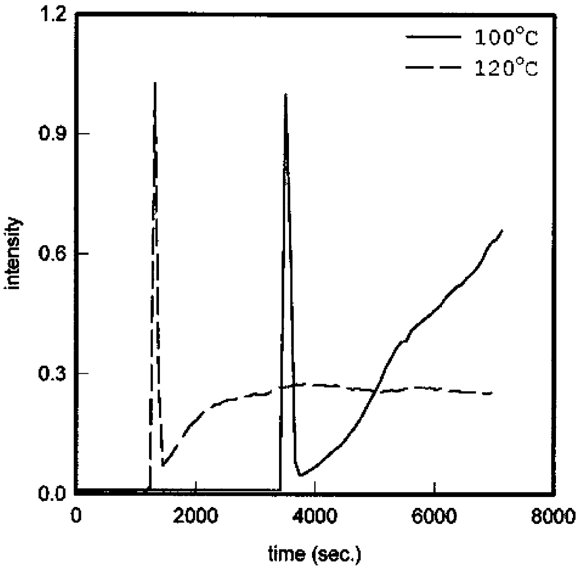

Fig. 10. Intensity variation with time at a fixed angle (ca. 20°) for the DGEBA/MDA/R45EPI (50/25.4/50) mixture at 100 and 120 °C.

characterized by Fig. 9(b) or (c). In these cases, relaxation is equivalent to the quenching effect (b) or dominant over the quenching effect (c). The scattering maximum will either remain the same as in (b) or decrease as is usual in phase separation without the presence of chemical reaction (c). It may be inferred that pattern formation in PIPS results from a competition between the reaction driven effect, which tends to reduce the length scale, and the thermally driven structural relaxation that favors domain growth. The DGEBA/MDA/R45EPI (70/25.7/30) mixture at a reaction temperature of 100 °C demonstrates no temporal dependence of q_{m} as depicted in Fig. 9(b), remaining nearly constant during the course of phase separation. On the other hand, the same mixture experiencing reaction conditions above 120 °C possesses a temporal variation of q_{m} depicted by Fig. 9(c). The increase in reaction temperature clearly imposes a stronger effect on structure relaxation over the rate of the self-condensation of DGEBA. The average domain size grows with time, as characterized by a decrease in q_{m}. This effect is more pronounced as the reaction temperature increases.

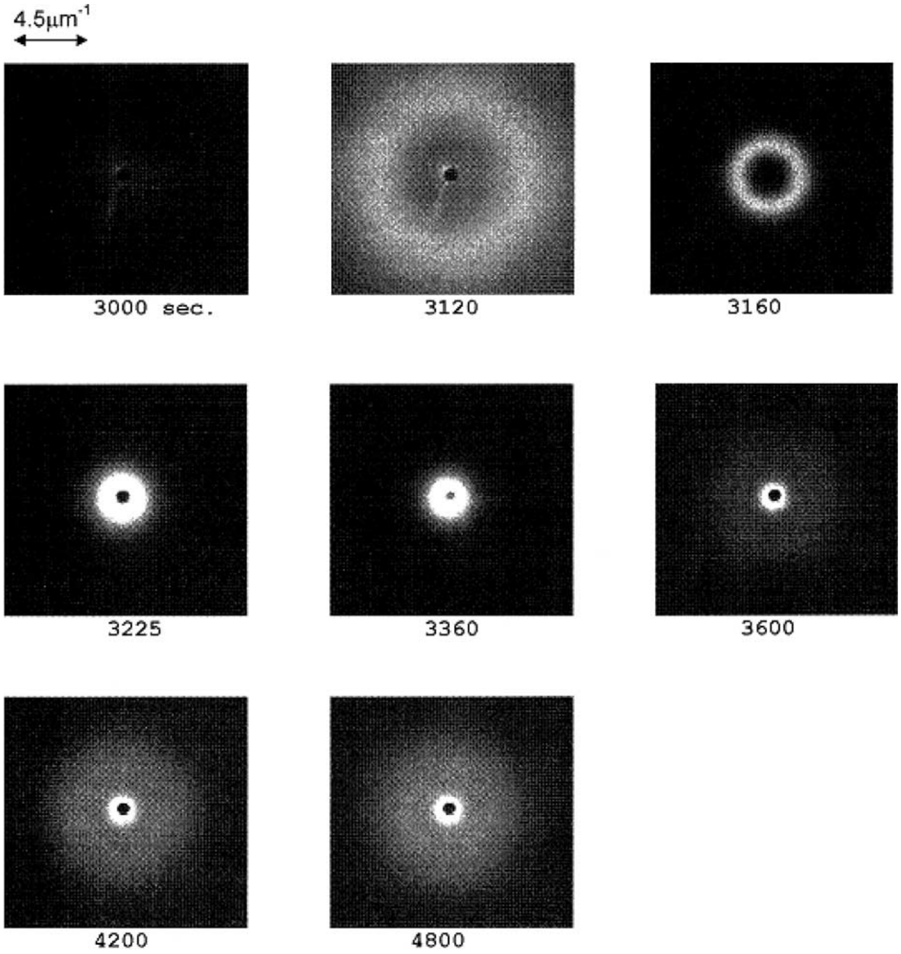

Fig. 11. Time evolution of scattering patterns of DGEBA/MDA/R45EPI (50/25.4/50) mixture at 100 °C, showing first phase separation, phase dissolution and subsequent second phase separation.

3.3. Dynamics of phase separation in the DGEBA/MDA/R45-EPI (50/25.4/50) mixture

The temporal variation of the scattered light intensity at a fixed arbitrary angle (approximately 20°) for the DGEBA/MDA/R45EPI (50/25.4/50) mixture for two reaction conditions is plotted in Fig. 10. Interestingly, for both conditions, the scattered light intensity abruptly increases first and then declines back to the almost initial value, followed by a subsequent steady increase. This observed trend occurs faster with an increase in the reaction temperature. This type of scattered light intensity variation has not been observed in conventional thermally quenched systems and thus deserves closer scrutiny.

In an effort to understand this unusual behavior, time-resolved light scattering experiments were undertaken for the DGEBA/MDA/R45EPI (50/25.4/50) mixture. Fig. 11 demonstrates the temporal evolution of the scattering halo during the course of the reaction in the DGEBA/MDA/R45EPI (50/25.4/50) at 100 °C. It is striking to discern the unusual behavior exhibited by the reacting mixture, i.e. the scattering halo develops around 3000 s and intensifies for some period (3120 s) while the ring collapses to a smaller diameter (3160 s) with elapsed time. This stage corresponds to the growth of phase-separated domains. Subsequently, the scattering diminishes (3325–3360 s) which may be attributed to phase dissolution. Another interesting feature is the development of a new scattering peak (or shoulder to be precise) at a higher scattering angle that intensifies with time. This process is characterized as the occurrence of a secondary cascading phase separation.

The same phenomena can be identified in the snap-shots displaying the emerging phase-separated microstructures of Fig. 12. The structure is reminiscent of spinodally decomposed

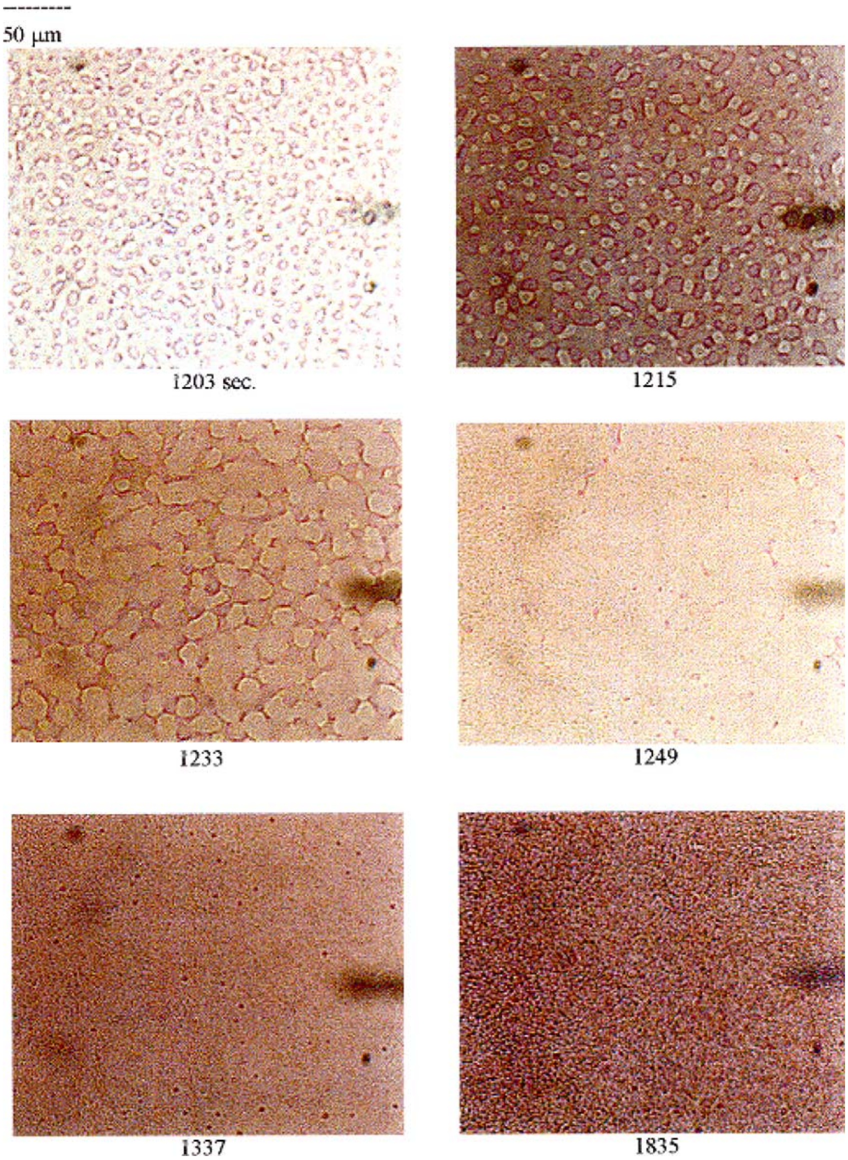

Fig. 12. Optical micrographs of DGEBA/MDA/R45EPI (50/25.4/50) mixture at 120 °C, showing first phase separation, virtual phase dissolution and subsequent second phase separation.

texture, although by no means a proof. This observation is not surprising in view of the fact that the 50/50 DGEBA/R45EPI is closer to the critical concentration. The SD like structure grows with elapsed time. Subsequently, the picture of the emerging structures shows drastic reduction in contrast, followed by a virtual disappearance of the growing domains. This stage is analogous to a phase dissolution process. Later, one can notice the emergence of smaller domains which may be characterized as the second phase separation.

A similar observation was made in the time-resolved light scattering at a reaction temperature of 120 °C (picture not shown here because the analysis will be made based on the scattering profiles). The scattered light intensity increases with time initially while q_m concurrently shifts to a smaller angle. It should be emphasized that the time scales for this phenomena under both reaction temperatures are remarkably different. An abrupt increase in scattering intensity occurs in nearly a third of the time of the 100 °C system condition at a higher reaction temperature of 120 °C. Specifically, phase separation occurs faster in 1150 s at 120 °C as opposed to 3120 s at 100 °C, further indicating that an increase in system temperature expedites structural relaxation. The scattered light intensity eventually decays without any noticeable change of q_m and this decrease is quite rapid. After the scattered light intensity reaches a minimum, it starts to increase again at somewhat larger q_m compared to the first scattering peak. This second scattering peak apparently does not change in position while the scattering intensity increases due to enhanced concentration fluctuations.

The time variations of I_m and q_m during this time period are illustrated in Fig. 13(a) and (b), respectively, for the two temperatures of 100 and 120 °C. The slope changes from $-1/3$ to -1, which is reminiscent of a thermal quenched system or that of a blend with low reactivity. The optical micrographs (pictures not shown) also demonstrate rapid growth of the structural domains during this time period. It may be concluded that the reaction rate is expedited by increases in the curing temperature, which in turn drives the phase transition processes such as phase separation, as well as a phase dissolution followed by a second phase separation, to proceed more quickly.

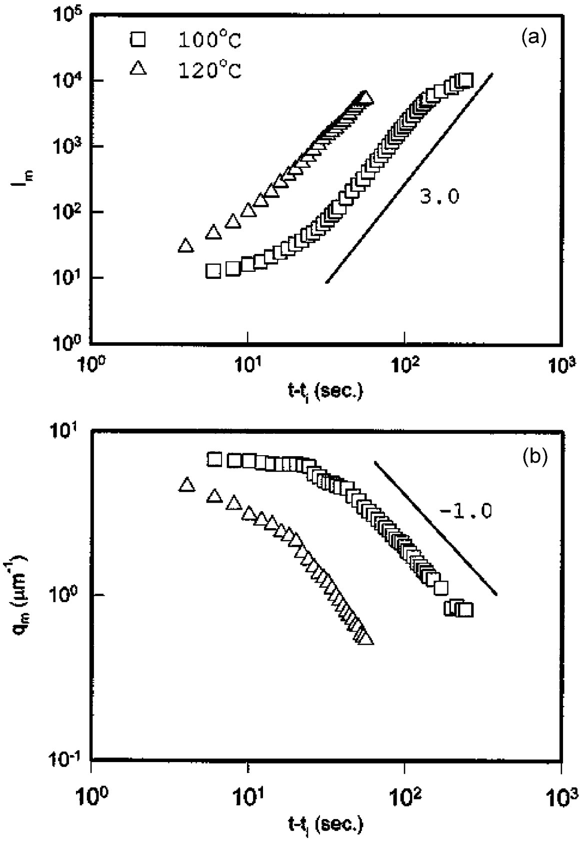

Fig. 13. Log–log plots of (a) maximum intensity (I_m) and (b) maximum wavenumber (q_m) vs. time for the DGEBA/MDA/R45RPI (50/25.4/50) mixture at 100 and 120 °C, respectively.

As discussed earlier, DSC scans of the DGEBA/MDA/R45-EPI mixtures show two characteristic peaks corresponding to the curing of DGEBA with MDA and the cross-reaction of DGEBA with R45EPI. The reaction of DGEBA with R45EPI was most pronounced in the DGEBA/MDA/R45EPI (50/25.4/50) mixture. Based on the DSC analysis, it is postulated that the condensation of DGEBA/MDA occurs first that in turn drives phase separation between the two constituent polymers. The crosslink density of the reacted DGEBA is expected to be low owing to a dilution effect resulting from the existence of R45EPI in the growing DGEBA regions since the mixture is initially miscible. The R45EPI molecules trapped in the networks may migrate out and react with growing DGEBA or residual DGEBA, if any, at the interface, resulting in phase dissolution. In practice, any copolymerization reaction cannot be expected to be complete, and thus the second phase separation between the copolymer (growing DGEBA-R45EPI) and R45EPI or growing DGEBA would occur. The present finding is in line with the observation by Brinke and co-workers who reported that a transesterification reaction between PC and polyesters such as PET and PAr ceases the growth of concentration fluctuation if the chemical reaction is faster than the phase separation [20].

If this scenario is accountable for the phase separation mechanism of the DGEBA/MDA/R5EPI (50/25.4/50) mixtures, the DGEBA/R45EPI (70/30) mixture having a reduced amount of curing agent may be able to exhibit the same phenomena observed in the DGEBA/MDA/R5EPI (50/25.4/50) mixture. In other words, the emerging DGEBA molecules would have an increased chance to copolymerize with the R45EPI molecules by reducing the amount of curing agent.

3.4. *Effect of the amount of curing agent*

In Section 3.3, it was postulated that a reduction in curing agent may provide the epoxy functional groups of DGEBA molecules a greater chance to react with the hydroxyl groups in the R45EPI molecules, i.e. copolymerization may occur favoring homogenization due to the possible compatibilization effect. It should be pointed out that the 70/25.7/30 mixture did not exhibit the phase dissolution phenomena. It can be

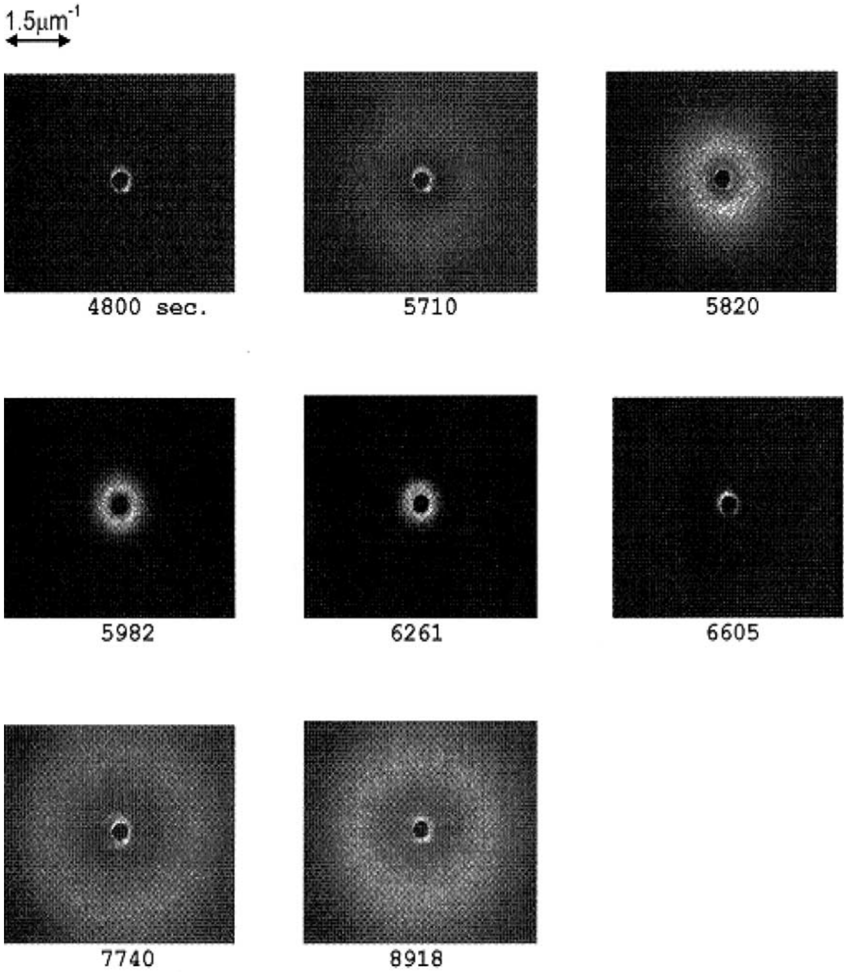

Fig. 14. Scattering patterns of DGEBA/MDA/R45EPI (70/6.4/30) mixture at 120 °C, showing first phase separation, phase dissolution and subsequent second phase separation.

anticipated that the above mixture may behave similarly to the 50/25.4/50 mixture, if the MDA concentration were reduced. Fig. 14 shows the time evolution of the scattering patterns for a DGEBA/MDA/R45EPI (70/6.4/30) mixture that contains one-fourth of the equivalent amount of curing agent. The scattered light intensity initially increases while the halo collapses to low scattering angles. Subsequently, the scattering pattern virtually disappears, suggestive of the anticipated phase dissolution behavior. A newer halo develops again at a larger scattering angle indicating the secondary phase separation. The scattering halo intensifies, while gradually shifting to a lower scattering angle due to the growth of the cascading phase-separated domains.

The temporal dependencies of I_m and q_m characterizing the two halos of the initial and secondary phase separation are depicted in Fig. 15(a) and (b), respectively. The slopes of -1 and $-1/3$ are observed for α in the first and second phase separation peaks of the DGEBA/MDA/R45EPI (70/6.4/30) mixture at 120 °C. Correspondingly, the values of 3 and 1 were obtained for β. This observed behavior is unusual and completely different from the thermal quenched systems [15,17], where the cluster dynamics occur with the growth exponent of $-1/3$ in the intermediate stage, which is accompanied by the percolation regime with the growth exponent of -1 in the late stages. It appears that the first phase transition behavior may be attributed to the consequence that the rate of reaction is low initially due to the deficient amount of the MDA utilized, and therefore it is dominated by the structure relaxation due to the thermal induced effect. It should also be recognized that all observed phenomena in this system occur at much longer time scales since the condensation of DGEBA/MDA is significantly slower. The reduction in MDA may raise the probability of collision between DGEBA and R45EPI, which in turn favors the cross-reaction to form a copolymer of DGEBA/R45EPI. The emerged copolymer at the domain interface may contribute to homogenization leading to phase dissolution. Subsequently, the second phase separation occurs at a slower speed with the growth exponent of $-1/3$ relative to the first phase separation, which is seemingly influenced by both partial (incomplete) curing of DGEBA/MDA and increased compatibilization effect from the copolymerization. It is reasonable to infer that the growth behavior in the intermediate and late stages of the present reaction-induced phase separation is strongly influenced by the concentration of the curing agent, MDA. Evidently, the effect of chemical cross-linking on the structural growth is most

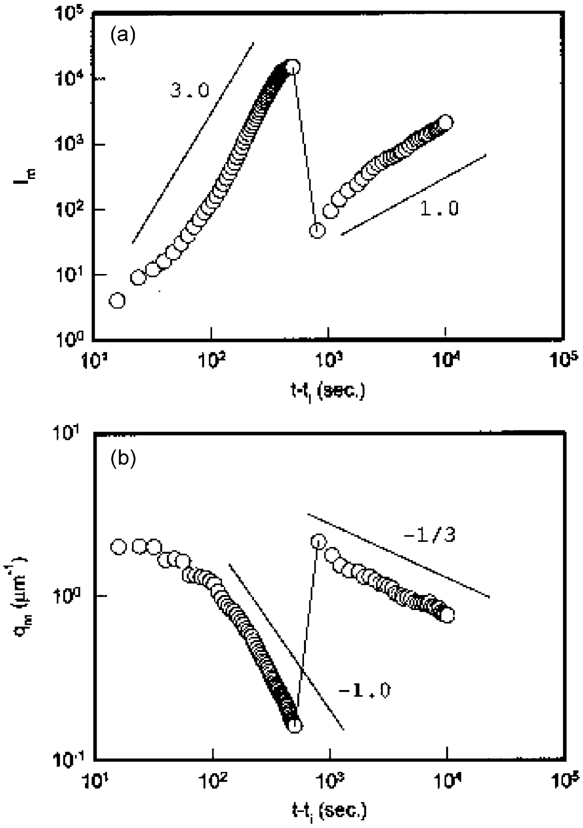

Fig. 15. Log–log plot of (a) intensity maximum (I_m) and (b) wavenumber maximum (q_m) vs. time for the DGEBA/MDA/R45EPI (70/6.4/30) mixture at 120 °C, showing the growth exponents ($-\alpha$ and β) of the initial phase separation (-1 and 3) and second phase separation ($-1/3$ and 1).

pronounced when the amount of the curing agent is adequately high.

4. Conclusions

We have demonstrated the existence of an unusual phase dissolution behavior in a system where both of the species, DGEBA and R45EPI, are reactive. This phenomenon is characterized by an initial phase separation caused by the dominant condensation of DGEBA/MDA thrusting the initially miscible system into the temporally dependent coexistence region of the phase diagram. At a certain time, either when the curing agent is nearly consumed or the resultant copolymer from a cross-reaction between the two species reaches a critical level, interfacial regions become diffuse, the amplitude of concentration fluctuations decrease, causing the disappearance of structure known as the phase dissolution. It was demonstrated that by changing the conditions of the reacting system, it is possible to change the balance between the size reduction (i.e. quenching effect), which is caused by chemical crosslinking of structure in the early stages yielding the peak shift q_m to a higher scattering angle, and the thermal relaxation of the system where structures grow resulting in a decrease in q_m. Altering the reaction temperature results in a greater effect on structural relaxation due to the domination of the thermal induced effect relative to that of the chemical reaction induced phenomenon. Careful selection of the reaction temperature and initial composition of the mixture provides one with greater control over the chemical architecture, allowing for morphological selection that would directly influence the mechanical properties of the end product.

Acknowledgements

Support of this work by the National Science Foundation NSF-DMR 02-09727 and the Ohio Board of Regents through a Research Challenge Grant.

References

[1] Bucknall CB. Toughened plastics. Appl Sci Publ 1977.
[2] Pearson RA, Yee AF. J Mater Sci 1986;21:2475.
[3] Bucknall CB, Partridge IK. Polymer 1989;30:213.
[4] Inoue T. Prog Polym Sci 1995;20:129.
[5] Williams RJJ, Rozenberg BA, Pascault JP. Adv Polym Sci 1997;128:95.
[6] Rosenberg BA, Sigalov GM, editors. Heterophase network polymers: synthesis, characterization and properties. London: Taylor & Francis; 2002.
[7] Kyu T, Lee J. Phys Rev Lett 1996;76:3746.
[8] Olabisi O, Rebeson LM, Shaw MT. Polymer–polymer miscibility. New York: Academic Press; 1979.
[9] de Gennes PG. J Chem Phys 1980;72:4756.
[10] Lifshitz IM, Slyozov VV. J Phys Chem Solids 1961;19:35.
[11] Langer JS, Bar-on M, Miller HD. Phys Rev A 1975;11:1417.
[12] Gunton JD, San Miguel M, Sahni PS. In: Domb C, Lebowitz JL, editors. Phase transitions and critical phenomena. New York: Academic Press; 1983 [chapter 3].
[13] Kawasaki K, Ohta T. Prog Theor Phys 1978;59:362.
[14] Siggia ED. Phys Rev A 1979;20:595.
[15] Binder K. Phys Rev B 1977;15:4425.
[16] Hashimoto T, Itakura M, Shimidzu N. J Chem Phys 1986;85:6773.
[17] Binder K, Stauffer D. Phys Rev Lett 1974;33:1006.
[18] Snyder HL, Meakin P. J Chem Phys 1983;79:5588.
[19] Furukawa H. Phys Lett A 1983;98:28.
[20] Brinke GT, Karasz FE, MacKnight WJ. Macromolecules 1983;16:1827.